Journal of Colloid and Interface Science 448 (2015) 315–319

Contents lists available at ScienceDirect

Journal of Colloid and Interface Science

www.elsevier.com/locate/jcis

Enhancing performance of P3HT:TiO_2 solar cells using doped and surface modified TiO_2 nanorods

Yu-Chieh Tu [a], Herman Lim [a], Chun-Yu Chang [a], Jing-Jong Shyue [a,b], Wei-Fang Su [a,*]

[a] No. 1, Sec. 4, Roosevelt Road, Department of Materials Science and Engineering, National Taiwan University, Taipei 10617, Taiwan
[b] No. 128, Sec. 2, Academia Road, Research Center for Applied Sciences, Academia Sinica, Taipei 11529, Taiwan

GRAPHICAL ABSTRACT

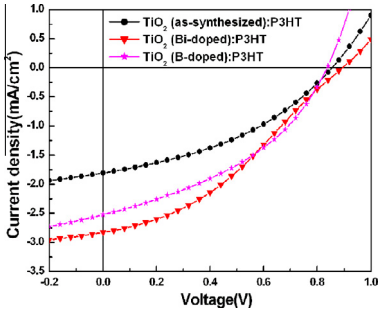

ARTICLE INFO

Article history:
Received 1 November 2014
Accepted 7 February 2015
Available online 19 February 2015

Keywords:
P3HT
TiO_2
Nanorods
Solar cell
Doping
Polymer

ABSTRACT

Here we demonstrated an approach to increase performance of P3HT:TiO_2 solar cell either by electron deficient boron or electron rich bismuth doping into TiO_2 nanorods. The B doping increases the absorption, crystallinity and electron mobility of TiO_2 nanorods. The Bi-doped TiO_2 has higher J_{sc} as compared with B-doped TiO_2, mainly due to the improvement of electron density and increased absorption of TiO_2 nanorods. The devices were fabricated from TiO_2 nanorods being surface modified by organic dye W-4. The dye facilitates the bandgap alignment and compatibility between TiO_2 and P3HT. The power conversion efficiency of solar cell has been increased by 1.33 times and 1.30 times for Bi-doped TiO_2 and B-doped TiO_2, respectively, as compared with that of as-synthesized TiO_2. The results suggest the optical and electronic properties of TiO_2 can be tuned by various dopants to enhance the device performance.

1. Introduction

Recently, the use of fossil fuel has led to environmental problems such as acid rain and global climate change. Furthermore, non-renewable fossil fuel will face exhaustion problem in the near future. Therefore, scientists are looking for sustainable and environmental friendly energy sources, so called "solar energy" to solve the energy problem. In the search for efficient ways to convert solar energy into electricity, various types of solar cells have been developed. At present, solar cell technology has been advanced from silicon wafer based first generation solar cell such as silicon p–n junction solar cell to the second generation of thin-film solar cell such as amorphous silicon solar cell to the third generation of solar cell including polymer-based cells, quantum dot cells, and multi-junction cells [1]. Polymer solar cell is based on bulk heterojunction (BHJ) which has potential to become low-cost solar cell [2]. Generally, there are two types of polymer solar cells that have been intensively studied: (1) polymer-fullerene derivative cells and (2) polymer-semiconducting nanoparticle cells. High

* Corresponding author. Fax: +886 2 23634562.
E-mail address: suwf@ntu.edu.tw (W.-F. Su).

http://dx.doi.org/10.1016/j.jcis.2015.02.015
0021-9797/

power conversion efficiency (PCE) has been achieved for poly(3-hexylthiophene) (P3HT) and [6,6]-phenyl C_{61}-butyric acid methyl ester (PCBM) based solar cell [3,4]. However, this type solar cell has thermal stability problem [5]. Therefore, we study a more stable solar cell of P3HT:TiO_2 and improve its PCE by using boron-doped TiO_2 and bismuth-doped TiO_2. The low cell efficiency of P3HT:TiO_2 system is due to its low short-circuit current (J_{sc}) and poor compatibility between P3HT and TiO_2. The short-circuit current of P3HT:TiO_2 is directly correlated to the mobility and current density of charges. The charge mobility of TiO_2 is one to two orders of magnitude lower than that of P3HT [6]. Both boron-doped TiO_2 and bismuth-doped TiO_2 have been studied extensively to increase the photocatalytic property of anatase TiO_2 [7,8]. Here we demonstrated two approaches to improve the electronic properties of TiO_2 for enhancing the performance of P3HT:TiO_2 solar cell: (1) to increase the electron mobility of TiO_2 by boron doping [9] and (2) to increase the electron density of TiO_2 by bismuth doping [10]. The TiO_2 nanorods were used in this study. The surface of TiO_2 nanorods was modified using 2-cyano-3-(5-(7-(thiophen-2-yl)-2,1,3-benzothiadiazol-4-yl)thiophen-2-yl) acrylic acid (W4) to be compatible and energy aligned with P3HT for efficient charge separation and transport [11–13].

2. Experimental

2.1. Materials

Some of the chemicals were used as received without any further purification including oleic acid (OA, 99%, Aldrich), pyridine (99%, Acros), titanium tetraisopropoxide (TTIP, 98%, Aldrich), boron n-butoxide (98%, Aldrich), trimethylamino-N-oxide dehydrate (TMNO, 98%, Acros), methanol (99%, Acros), and hexane (95%, J.T. Baker).

2.2. Synthesis and surface modification of doped TiO_2 nanorods

2.2.1. As-synthesized TiO_2 nanorods

We first synthesized TiO_2 nanorods by hydrolyzing TTIP according to literature [9] and call it as-synthesized TiO_2 nanorods (as-synthesized TiO_2). The procedure typically involved by placing 180 g of oleic acid in a 250 ml three-neck flask, heated it to 120 °C for one hr in Ar and then cooled down to 98 °C. Followed by 7.5 ml of TTIP was injected into the reaction flask and mixed well, then a mixture solution of 5.7 g of trimethylamine-N-oxide dehydrate and 25 g of H_2O was injected into the reaction flask, the reaction was carried out at 98 °C for 9 h in Ar which yielded as synthesized TiO_2 nanorods.

2.2.2. B-doped TiO_2 nanorods

The similar procedure of as synthesized TiO_2 nanorods described above was used but by replacing 0.7 at.% Ti with B using boron n-butoxide instead of TTIP according to literature [9].

2.2.3. Bi-doped TiO_2 nanorods

The bismuth isopropoxide [14] was firstly synthesized and used as bismuth dopant in the sol–gel synthesis of TiO_2 nanorods. Sodium (1.2 g, 0.052 mol) was charged into a 250 ml three-neck reaction flask equipped with a condenser, the flask was then evacuated and refilled with Ar. Dried THF (70 ml) and dry isopropyl alcohol (3.3 ml, 0.043 mol) were transferred to the reaction flask by using double tips needle under argon purging. The temperature was brought to 70 °C and held for 12 h under argon purging to obtain sodium isopropoxide. Separately, bismuth trichloride (4.7 g, 0.15 mol) were charged into a 250 ml reaction flask and evacuated for overnight and then refilled with argon. Dried THF (70 ml) was transferred to the reaction flask and the suspension was stirred at 40 °C for at least 1 h to make bismuth trichloride solution. After the sodium-isopropoxide solution was cooled to room temperature, the bismuth trichloride solution was transferred using double tips needle under argon purging. The solution was stirred for 8 h at 45 °C and then cooled to room temperature and THF was distilled off under vacuum. Dry hexane was then added to dissolve the product and the filtrate was collected under argon purged. After the hexane was removed, the brown solid of bismuth isopropoxide was collected and stored under argon. ^{1}H NMR (MeOD, 400 MHz) δ = 3.84 ppm (3H, m), 1.07 ppm (18H, d). Finally, the same procedure of as synthesized TiO_2 was used to synthesize Bi doped TiO_2 but by replacing 0.02 at.% Ti with Bi using bismuth isopropoxide instead of TTIP described above.

2.2.4. Surface modification of TiO_2 nanorods

The surface modification experiments were followed by the procedures reported in literatures [11,13]. First, the above synthesized three kinds of TiO_2 nanorods were precipitated and washed 4 times with methanol to remove excess oleic acid. Then, these TiO_2 nanorods were treated with pyridine by refluxing at 70 °C for 24 h in Ar to remove oleic acid further. These pyridine modified TiO_2 nanorods were ligand exchanged with W4-dye molecule by dissolving the dye powder in the pyridine solution of TiO_2 and refluxing at 70 °C for 24 h in Ar to obtain W4-dye modified TiO_2 nanorods.

2.3. Characterization of TiO_2 nanorods

The crystal structure of TiO_2 nanorods was determined by X-ray diffraction (XRD) (Rigaku, TTRAX III). XRD patterns were collected from 2θ between 20° and 80° with a 0.005° step at 5° min^{-1}. The phase identification of anatase TiO_2 was confirmed by comparing with JCPDS database. The 150 mg of each sample was used for XRD to quantify the sample crystallinity by calculating the intensity of XRD peaks. The UV–Vis spectra of different TiO_2 nanorods were obtained using Perkin Elmer Lambda 35 UV/Vis spectrometer at a concentration of 1 mg of TiO_2 nanorods in 7 ml of pyridine. The particle size and selected-area electron diffraction (SAED) of the TiO_2 were studied by transmission electron microscopy (TEM) (FEI TecnaiG2 F20) at 200 keV. Thermogravimetric analysis (TGA) (TA Instrument, SDT-Q600) was performed from room temperature to 525 °C at 20 °C min^{-1} in air to determine the quantity of OA on TiO_2. The X-ray photoelectron spectroscopy (XPS) (ULVACPHI, Chigasaki) was used to determine the surface chemistry of TiO_2 by calculating the binding energy of the emitted electrons. The electron mobility of all three differently synthesized types of TiO_2 nanorods was obtained by the space charge limited current (SCLC) method [15].

2.4. Synthesis and characterization of P3HT

The synthesis of P3HT polymer was carried out by modified McCullough polymerization [16]. The monomer 2,5-dibromo 3-hexylthiophene was first synthesized [16] (4 g, 0.0126 mol) and placed into a three-neck reaction flask equipped with a condenser and evacuated for at least 1 h before refilling with N_2 and adding dried THF (240 ml). The mixture was cooled with an ice bath and isopropyl magnesium chloride (5.88 ml, 0.0117 mol) was added by air-tight syringe and allowed to react for 1 h in ice bath. Ni(dppe)Cl_2 (0.022 g, 0.042 mmol) was added to the reaction mixture in dried THF at 0 °C and warmed to 45 °C immediately with vigorous stirring. The reaction color was changed from pale yellow to reddish orange implying the polymerization was taking place. The polymerization was continued for 30 min before terminated

with methanol (5 ml) and precipitated into methanol. The solid was collected and Soxhlet subsequently with methanol, hexane and extracted with chloroform. M_w = 58037 (1.39), 1.5 g (yield = 73.6%) and regioregularity = 96.5%. Regioregularity of washed P3HT as calculated from ^{1}H NMR spectra (supporting information Fig. S1) was 96.5%.

3. Results and discussion

Three types of TiO_2 nanorods were synthesized in our laboratory for this study: TiO_2 (as-synthesized), TiO_2 (B-doped) and TiO_2 (Bi-doped). The concentration of each dopant was optimized to have the highest crystallinity in the doped TiO_2 where B was 0.7 at.% and Bi was 0.02 at.%. The high crystallinity of TiO_2 is expected to have high charge mobility [9]. The XRD patterns of all three TiO_2 nanorods are shown in Fig. 1. They all exhibit anatase structure (JCPDS No. 782486) without any secondary phase; however, the peaks are rather broad as compared with the standard micro size sample from JCPDS due to the large surface scattering of nanoparticles [17]. The formation of nanorods is confirmed due to the peak ratio of (004) to (200) is more than 2 which is the characteristic of nanorods. In general, for the spherical particles, the ratio is less than 1 as shown in the JCPDS standard TiO_2 (Fig. 1).

The boron or bismuth concentration was too low to be detected. The intensity of the (101) peak was used to determine the extent of crystallinity for each sample. The weight of each sample was controlled to be the same to avoid any discrepancy. The results indicate the extent of crystallinity of different samples is TiO_2

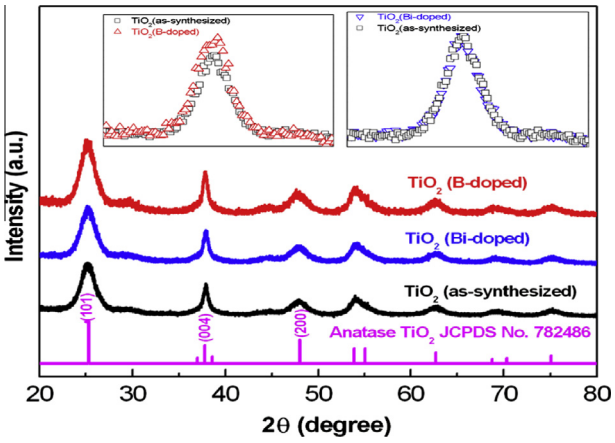

Fig. 1. XRD patterns of different TiO_2.

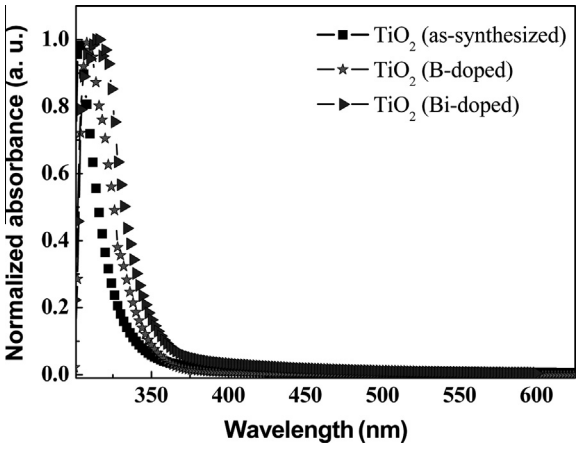

Fig. 2. UV–Vis spectra of different TiO_2 nanorods.

Table 1
Characteristics of different TiO_2 nanorods.

Sample	Size by TEM (nm)		Wt.% of oleic acid	Electron mobility ($cm^2/V\,s$)
	width	length		
TiO_2 (as-synthesized)	4 ± 1	33 ± 4	30.6	2.46×10^{-5}
TiO_2 (B-doped)	4 ± 2	35 ± 6	29.3	5.27×10^{-4}
TiO_2 (Bi-doped)	4 ± 2	38 ± 5	25.1	2.32×10^{-5}

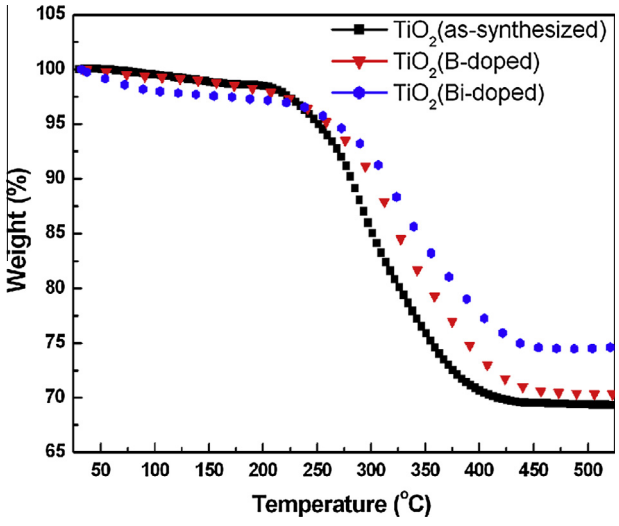

Fig. 4. TGA analysis of different types TiO_2 nanorods.

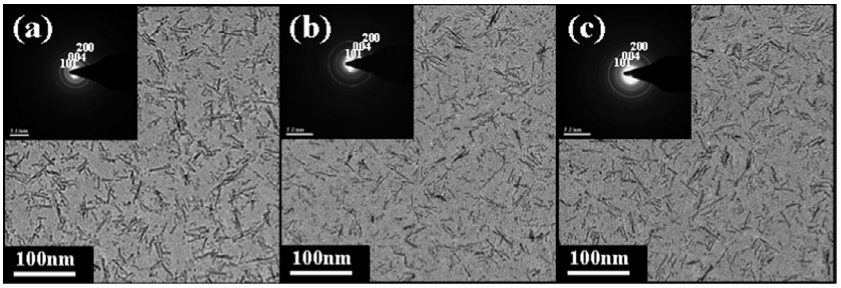

Fig. 3. TEM images of different TiO_2 nanorods (a) TiO_2 (as-synthesized), (b) TiO_2 (B-doped), and (C) TiO_2 (Bi-doped). The insert shows the SAED patterns obtained from the image area.

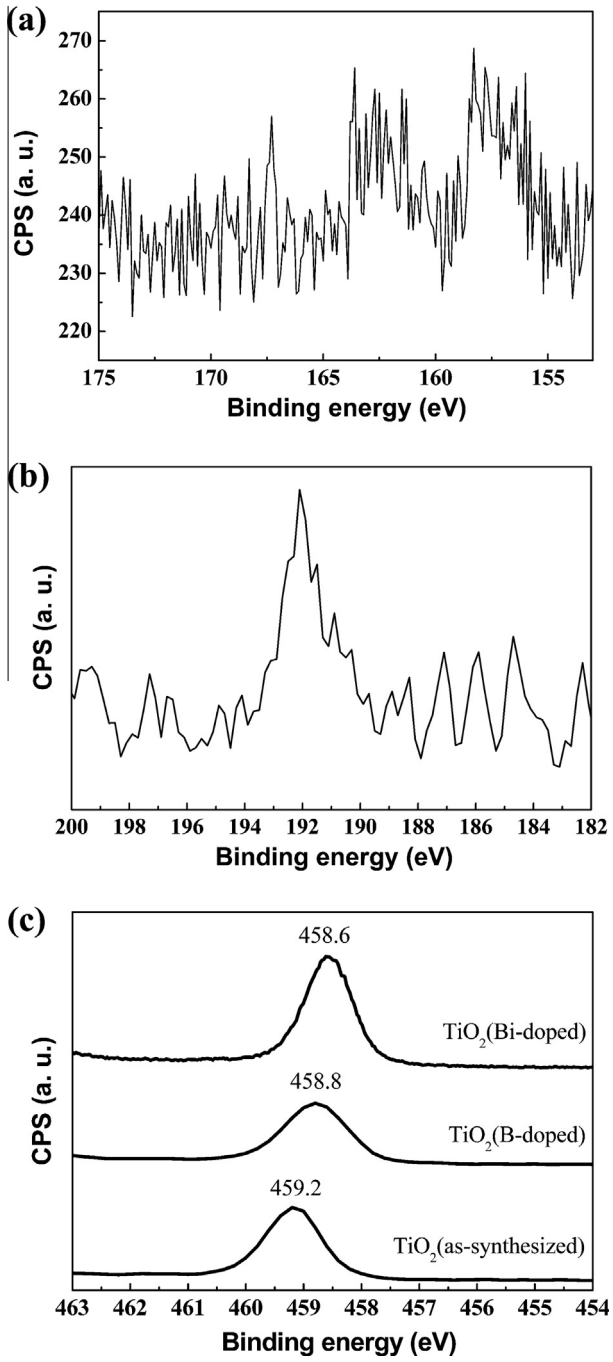

Fig. 5. XPS spectra of (a) Bi $4f^{7/2}$ low binding energy (158 eV) and $4f^{5/2}$ high binding energy (163 eV) of Bi-doped TiO_2, and (b) B1s binding energy of B-doped TiO_2 (c) Ti $2p^{3/2}$ binding for different TiO_2 nanorods.

(B-doped) > TiO_2 (as-synthesized) ~ TiO_2 (Bi-doped). The TiO_2 (B-doped) has the best crystallinity which may due to the different in ionic radius with B^{3+} (0.02 nm) being smaller than the Ti^{4+} (0.06 nm) ion. The boron atoms can be easily present in the matrix of TiO_2 as nucleus for good crystal growth.

Fig. 2 shows the comparison of UV–Vis spectra of different TiO_2 nanorods. The results indicate that the doping of B or Bi induces a red shift in absorption. The largest red shift is observed for TiO_2 (Bi-doped), implying the successful incorporation of the bismuth atom into the TiO_2 lattice. Both TiO_2 (B-doped) and TiO_2 (Bi-doped) can reduce the valence of the titanium ion from Ti^{4+} to Ti^{3+} (more detailed discussions shown in below) [9,18].

Fig. 3 shows the TEM images of three different kinds of TiO_2 nanorods. The dimensions of nanorods are summarized in Table 1. The TiO_2 nanorods are relatively uniform in size (approx. 5 nm × 35 nm). From the SAED patterns, bismuth and boron doping do not alter the crystal phase of anatase TiO_2. Both dopants increase the diameter slightly and length of TiO_2 nanorods. It is interesting to note that the size of Bi doped TiO_2 is the largest. The cause is not clear this time.

The amounts of OA on different TiO_2 nanorods were determined by TGA. The curves are plotted in Fig. 4 and the results are summarized in Table 1. Among the samples, the TiO_2 (Bi-doped) contains the least amount of OA, the result is in good agreement with its larger size and less surface area as compared with other samples.

The XPS was used to characterize the doping in TiO_2 nanorods. Three XPS studies were performed for Bi dopant, B dopant and pristine TiO_2 respectively. Fig. 5a clearly shows the presence of Bi dopant with two peaks: the low binding energy peak of 158 eV for Bi $4f^{7/2}$ and the high energy peak of 163 eV for Bi $4f^{5/2}$ which are related to the Bi–O bonding [19]. According to the binding energy of B in TiB_2 (Ti–B: 187.5 eV) and B_2O_3 (B–O: 193.0 eV) [9], the B 1s binding energy of 192.1 eV may be assigned to either Ti–O–B bond or O–Ti–B bond for TiO_2 (B-doped) as shown in Fig. 5(b). Compared with the Ti $2p^{3/2}$ binding energy of as-synthesized TiO_2 (459.2 eV), the other two kinds of TiO_2 decrease to lower binding energy (458.8 eV for B-doped TiO_2 and 458.6 eV for Bi-doped TiO_2) as shown in Fig. 5(c). The result shows the Ti^{4+} is partially reduced with delocalized electrons by electron transfer from the boron or bismuth dopant. There is a more shift to the lower energy as Bi was doped to TiO_2 which show that the presence of Bi increase the electron density around Ti.

The SCLC method was used to determine the electron mobility of different TiO_2 nanorods. The TiO_2 (B-doped) exhibits the highest electron mobility among three kinds of TiO_2 as shown in Fig. 6. The main causes are the partially reduction of Ti^{4+} by boron and the improved crystalline structure of TiO_2 nanorods [9].

To assess the photovoltaic performance of different kinds of TiO_2 nanorods, we prepared P3HT:TiO_2 solar cells using these three different types of TiO_2 nanorods that we have synthesized and characterized. The devices consist of six layers with the structure of indium-tin-oxide (ITO)/poly (3,4-ethylenedioxythiophene) (PEDOT:PSS)/P3HT/P3HT:TiO_2/TiO_2 nanorods/Al. From our previous studies [12,13], we demonstrated that W4-dye modified TiO_2 can improve the efficiency of P3HT:TiO_2 solar cells due to the aligned bandgap and improved compatibility between P3HT and TiO_2. Thus, we used W-4 modified TiO_2 to fabricate solar cells in

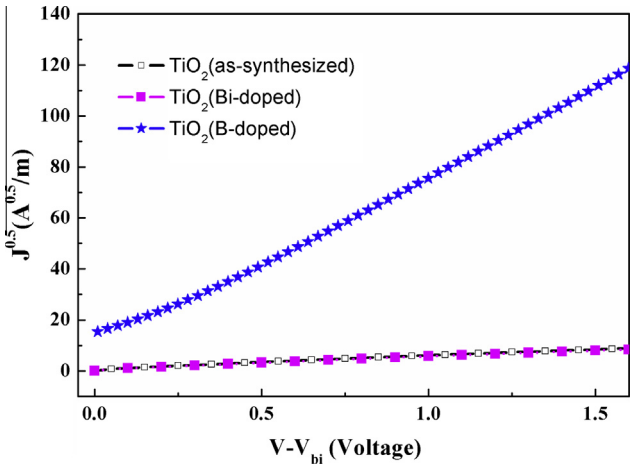

Fig. 6. Electron mobility in different TiO_2 nanorods measured by space charge limited current (SCLC) method.

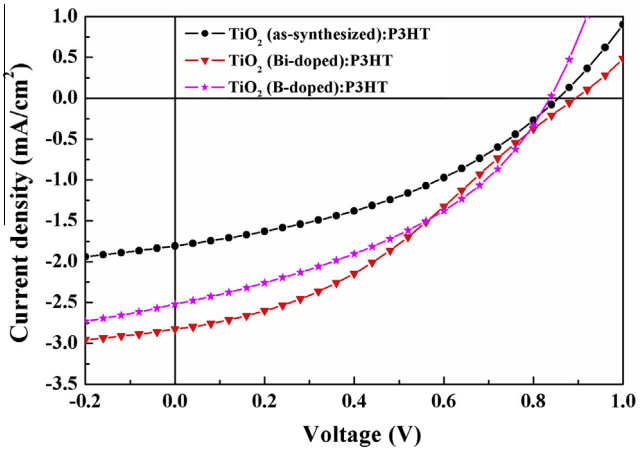

Fig. 7. *I–V* curve of P3HT:TiO_2 solar cells fabricated from different W4-dye modified TiO_2 nanorods.

Table 2
Performance of photovoltaic devices using different TiO_2 nanorods.

Sample	V_{oc}	J_{sc}	FF (%)	PCE (%)
TiO_2 (as-synthesized)	0.86 ± 0.02	1.80 ± 0.08	42.86 ± 2.77	0.67 ± 0.07
TiO_2 (B-doped)	0.83 ± 0.01	2.67 ± 0.13	39.24 ± 2.01	0.87 ± 0.07
TiO_2 (Bi-doped)	0.89 ± 0.01	2.81 ± 0.02	35.55 ± 0.45	0.89 ± 0.01

this study. The efficiency of the P3HT:TiO_2 solar cell has been increased by 1.30 times and 1.33 times for B-doped TiO_2 and Bi-doped TiO_2 respectively as compared with that of as-synthesized TiO_2 as shown in Fig. 7. The performance of these three kinds of solar cells is summarized in Table 2. The Bi-doped TiO_2 has shown the highest open-circuit voltage (V_{oc}) and short-circuit current (J_{sc}) as compared with as-synthesized TiO_2 and B-doped TiO_2 due to its higher electron density from the lone electron pairs of Bi. In summary, either B-doped TiO_2 or Bi-doped TiO_2 is a promising way for increasing the power conversion efficiency (PCE) of P3HT:TiO_2 solar cells.

4. Conclusion

We have successfully synthesized B-doped TiO_2 and Bi-doped TiO_2 by using a sol–gel method. The B-doped TiO_2 nanorods can increase crystallinity of as-synthesized TiO_2 in the grains and improve its electron mobility. The Bi-doped TiO_2 nanorods exhibit a slightly lower crystallinity compared with as-synthesized nanorods but Bi doping does result in a higher electron density as observed from XPS analysis. By improving the electron mobility and electron density of TiO_2 nanorods, one can increase the efficiency of the P3HT:TiO_2 solar cells fabricated from W4-dye modified TiO_2 nanorods by 1.30 times and 1.33 times for B-doped TiO_2 and Bi-doped TiO_2 respectively as compared with that of as-synthesized TiO_2. Both B-doped TiO_2 and Bi-doped TiO_2 point toward useful approaches for developing TiO_2:P3HT solar cell with high efficiency.

Acknowledgment

The authors thank the Ministry of Science and Technology of Taiwan (101-2120-M-002-003, and 102-3113-P-002-027) for financial support of this research.

Appendix A. Supplementary material

Supplementary data associated with this article can be found, in the online version, at http://dx.doi.org/10.1016/j.jcis.2015.02.015.

References

[1] C.-F. Lin, W.-F. Su, C.-I. Wu, I.-C. Cheng, Cheng, Organic, Inorganic and Hybrid Solar Cells: Principles and Practice, Wiley, 2012.
[2] C.J. Brabec, J.R. Durrant, MRS Bull. 33 (2008) 671.
[3] C.W. Liang, W.F. Su, L. Wang, Appl. Phys. Lett. 95 (2009) 133303.
[4] H.C. Liao, C.S. Tsao, T.H. Lin, C.M. Chuang, C.Y. Chen, U.S. Jeng, C.H. Su, Y.F. Chen, W.F. Su, J. Am. Chem. Soc. 133 (2011) 13064.
[5] Y.C. Huang, S.Y. Chuang, M.C. Wu, H.L. Chen, C.W. Chen, W.F. Su, J. Appl. Phys. 106 (2009) 034506.
[6] Y.C. Huang, W.C. Yen, Y.C. Liao, Y.C. Yu, C.C. Hsu, M.L. Ho, P.T. Chou, W.F. Su, Appl. Phys. Lett. 96 (2010) 123501.
[7] T. He, X. Guo, K. Zhang, Y. Feng, X. Wang, RSC Adv. 4 (2014) 5880.
[8] J. Ma, J. Chu, L. Qiang, J. Xue, RSC Adv. 2 (2012) 3753.
[9] Y.C. Tu, J.F. Lin, W.C. Lin, C.P. Liu, J.J. Shyue, W.F. Su, Cryst. Eng. Commun. 14 (2012) 4772.
[10] S. Bagwasi, B. Tian, J. Zhang, M. Nasir, Chem. Eng. J. 217 (2013) 108.
[11] Y.Y. Lin, T.H. Chu, S.S. Li, C.H. Chuang, C.H. Chang, W.F. Su, C.P. Chang, M.W. Chu, C.W. Chen, J. Am. Chem. Soc. 131 (2009) 3644.
[12] J. Yu, T.L. Shen, W.H. Weng, Y.C. Hang, C.I. Huang, W.F. Su, S.P. Pwei, K.C. Ho, L. Wang, Adv. Energy Mater. 2 (2012) 245.
[13] T.W. Zeng, C.C. Ho, Y.C. Tu, G.Y. Tu, L.Y. Wang, W.F. Su, Langmuir 27 (2011) 15255.
[14] W.F. Su, Y.T. Lu, Mater. Chem. Phys. 80 (2003) 632.
[15] P.N. Murgatroyd, J. Phys. D Appl. Phys. 3 (1970) 151.
[16] B. Pal, W.-C. Yen, J.-S. Yang, W.-F. Su, Macromolecules 40 (2007) 8189.
[17] A.S. Edelstein, R.C. Cammarata, Nanomaterials: Synthesis, Properties and Applications, Institute of Physics Publishing, Bristol and Philadelphia, 1996. p. 93.
[18] E. Finazzi, C.D. Valentin, G. Pacchioni, J. Phys. Chem. C 113 (2009) 220.
[19] M.A. Hughes, Y. Fedorenko, B. Gholipour, J. Yao, T.-H. Lee, R.M. Gwilliam, K.P. Homewood, S. Hinder, D.W. Hewak, S.R. Elliott, R.J. Curry, Nat. Commun. 5 (2014) 5346.